Published in final edited form as:
Dev Biol. 2007 May 15; 305(2): 389–396. doi:10.1016/j.ydbio.2007.02.025.

Conversion of midbodies into germ cell intercellular bridges

Michael P. Greenbaum[1,2], **Lang Ma**[1], and **Martin M. Matzuk**[1,2,3,*]

[1] Department of Pathology, Baylor College of Medicine, One Baylor Plaza, Houston, TX 77030

[2] Department of Molecular and Human Genetics, Baylor College of Medicine, One Baylor Plaza, Houston, TX 77030

[3] Department of Molecular and Cellular Biology, Baylor College of Medicine, One Baylor Plaza, Houston, TX 77030

Abstract

Whereas somatic cell cytokinesis resolves with abscission of the midbody, resulting in independent daughter cells, germ cell cytokinesis concludes with the formation of a stable intercellular bridge interconnecting daughter cells in a syncytium. While many proteins essential for abscission have been discovered, until recently, no proteins essential for mammalian germ cell intercellular bridge formation have been identified. Using TEX14 as a marker for the germ cell intercellular bridge, we show that TEX14 co-localizes with the centralspindlin complex, mitotic kinesin-like protein 1 (MKLP1) and male germ cell Rac GTPase-activating protein (MgcRacGAP), and converts these midbody matrix proteins into stable intercellular bridge components. In contrast, septins (SEPT) 2, 7, and 9 are transitional proteins in the newly forming bridge. In cultured somatic cells, TEX14 can localize to the midbody in the absence of other germ cell specific factors, suggesting that TEX14 serves to bridge the somatic cytokinesis machinery to other germ cell proteins to form a stable intercellular bridge essential for male reproduction.

Keywords

TEX14; intercellular bridge; cytoplasmic bridge; ring canal; knockout; centralspindlin; septins; midbody

Introduction

At the termination of cytokinesis, mammalian cells are connected transiently by an intercellular bridge preceding abscission (Fabbro et al., 2005; Fielding et al., 2005; Gromley et al., 2005; Low et al., 2003). In germ cells, these transient structures are transformed into stable intercellular bridges (Burgos and Fawcett, 1955; Dym and Fawcett, 1971; Fawcett et al., 1959; Weber and Russell, 1987), allowing the midbody and central spindle to break down without abscission via an unknown mechanism. Over a half century of microscopic studies have provided a detailed morphological description of intercellular bridges (Burgos and Fawcett, 1955; Dym and Fawcett, 1971; Fawcett et al., 1959; Huckins and Oakberg, 1978;

*Corresponding author: Martin M. Matzuk, MD. PhD., The Stuart A. Wallace Chair and Professor, Department of Pathology, Baylor College of Medicine, One Baylor Plaza, Houston, TX, 77030, Email: E-mail: mmatzuk@bcm.tmc.edu, Tel: 713-798-6451, FAX: 713-798-5833.

Moens and Hugenholtz, 1975; Ren and Russell, 1991; Ventela et al., 2003; Weber and Russell, 1987). Electron microscopy shows that germ cell cytokinesis initially appears identical to somatic cell cytokinesis, but at completion, an electron dense bridge density is seen lining the intercellular bridge after the midbody breaks down (Weber and Russell, 1987). The relationship between the germ cell-specific bridge density and the midbody has not been determined, and the process of mammalian germ cell intercellular bridge formation has not been described at the molecular level. Until the discovery of TEX14 (Greenbaum et al., 2006), proteins required for the germ cell intercellular bridge were unknown.

Germ cell intercellular bridges have been conserved over one billion years (Hedges, 2002) from invertebrates to humans (Fawcett et al., 1959) and are required for fertility in invertebrates (Brill et al., 2000; Hime et al., 1996; Robinson et al., 1994; Robinson and Cooley, 1996). In mammals, intercellular bridges connect hundreds of germ cells in a syncytium that is clonally derived from a single spermatogonial stem cell (Huckins, 1971). Loss of mammalian germ cell bridges prevents syncytium formation, disrupts spermatogenesis, and results in sterility (Greenbaum et al., 2006). In contrast to mammals, germ cell intercellular bridge formation has been described in molecular detail in *Drosophila*. Surprisingly, while key complexes essential for somatic cell cytokinesis are conserved in all cells from invertebrates from humans (Glotzer, 2005), germ cell intercellular bridges are compositionally different (Hime et al., 1996; Robinson and Cooley, 1996) and have different molecular requirements even between male and female *Drosophila* (Dodson et al., 1998). Given these interspecies differences, it appears that there may be multiple ways to form stable germ cell intercellular bridges.

Biochemical enrichment, followed by proteomic analysis of the enriched fraction, has become a valuable tool for studying the composition of large cellular structures (Yates et al., 2005). Multiple structures, including those related to cytokinesis, such as the midbody, mitotic spindle, and centrosome, have been studied with this approach (Skop et al., 2004; Yates et al., 2005), and these studies have resulted in a greater understanding the components of these structures and their potential functions. Herein, a proteomic approach was applied to intercellular bridges, demonstrating for the first time in mammals that intercellular bridges are formed from the midbody in a TEX14-dependent manner.

Materials and Methods

Enrichment of Intercellular Bridges

All steps are performed on ice or at 4 °C unless otherwise specified. Four milliliters of freshly prepared homogenization buffer [4mM HEPES, pH 7.5; 0.32M sucrose; Complete, Mini, EDTA-free (Roche, Basel, Switzerland)] are placed in a 10ml glass Potter-Elvehjem homogenizer (Wheaton, Millville, NJ) and stored on ice. Twelve 16-day-old CD1 male mice are sacrificed. As the animals were sacrificed, the testes are immediately dissected, and the tunica albuginea was removed. Ultra-fine dissecting scissors are used to quickly slice the tubules with about 40–50 quick cuts. The tubules are immediately transferred to the buffer in the homogenizer. Once all tubules are transferred (total time is about 25 minutes), they are homogenized by hand with 12 strokes of a Teflon pestle, creating a cloudy, light pink suspension. This total lysate is distributed equally into four 1.5ml microcentrifuge tubes (Eppendorf, Westbury, NY) and a 100ul sample is taken for western blot analysis. Samples are centrifuged at 720g in an Eppendorf 5417C microcentrifuge for 10 minutes. The supernatant (S1) is then transferred to new tubes and the pellet (P1) is discarded. The supernatant (S1) is centrifuged at 3,500g for 10 minutes. The supernatant (S2) is discarded and the each pellet (P2) is washed by resuspending in 500ul of homogenization buffer and centrifuging again for 10 minutes at 3,500g. The washed P2 pellets are resuspended in 250ul of lysis buffer [4mM HEPES, pH 7.5; 0.5% Triton X-100; Complete, Mini, EDTA-free (Roche)]. Ten percent, a 25ul aliquot is taken from each tube, combined, and kept for western blot analysis. An

additional 775ul of lysis buffer is added to each sample, and the samples are incubated 30 minutes on an orbital rocker at 4°C. The samples are then centrifuged again for 10 minutes at 3,500g. The final pellets (P3) are rinsed by gently overlaying 500ul of lysis buffer onto the pellet and centrifuging a final time for 5 minutes at 3,500g. The supernatant is completely removed, and the four P3 pellets are resuspended in a total of 100ul of lysis buffer for western blot analysis. Samples for western blot analysis were sonicated and protein concentration was measured with the BCA kit (Pierce).

Production of anti-TEX14 antibody

Antibodies to amino acids 885–1301 of the mouse TEX14 protein were generated in goat using methods described previously (Greenbaum et al., 2006), and affinity purified with the Aminolink Plus Immunobilization Kit (Pierce, Rockford, IL). Affinity purified antibodies had a final concentration of 1ug/ul.

Western blot analysis

Blots were incubated with primary antibodies at 4°C overnight at 1:2500 for goat anti-TEX14, 1:3000 for mouse anti-Beta Actin, 1:2000 for rabbit anti-GM130 and rabbit anti-SYCE1, and 1:1000 for rabbit anti-MKLP1, rabbit anti-MgcRacGAP, rabbit anti-SEPT2, rabbit anti-SEPT7, and rabbit anti-SEPT9. Secondary peroxidase conjugated antibodies (BioRad, Hercules, CA for rabbit, and Vector, Burlingame, CA for other species) were used at 1:5000. Western blots were detected with chemiluminescence (Amersham Biosciences, Buckinghamshire, England) and exposed to BioMax XAR film (Eastman Kodak, Rochester, NY) or on a Kodak Image Station 2000MM and quantified with Kodak MI software.

Cell culture

HeLa or Chinese Hamster ovary (CHO) K1 cells were grown in DMEM (10% fetal calf serum, 1% penicillin/streptomycin)(Invitrogen) on Poly-D-Lysine coated cover slips in 6 well culture plates (Corning, Corning, NY). Cells were transfected in 2 ml of fresh media with 1ug of pCMV-Tag2A (Stratagene, La Jolla, CA) containing the full mouse TEX14 open reading frame using 3ul of Fugene6 (Roche) as directed by the manufacturer.

Immunofluorescence analysis

Mouse testes, P3 pellets, and cell culture cover slips were fixed overnight at 4°C in 4% paraformaldehyde in TBS (100mM Tris-Cl, pH 7.5; 0.9%/150mM NaCl). Mouse testis were washed three times in 70% EtOH and then overnight at 4°C in 70%EtOH. They were then embedded in paraffin for sectioning. Five um section were cut and prepared for immunostaining as described previously (Greenbaum et al., 2006). P3 pellets and cover slips were washed three times for 20 minutes each in TBS. P3 pellets were then transferred to Superfrost/Plus slides (Fisher Scientific, Houston, TX) and allowed to air dry. A Bouins fixed human testis (18 years old) was purchased from Clonetech (now BD biosciences, Mountain View, CA). Samples were blocked in TBS, 3% BSA for 1 hour at room temperature. Antibodies were diluted in TBS plus 3% BSA and used for overnight incubation at 4°C at the following dilutions: mouse anti-beta tubulin T4026 (Sigma, St. Louis, Missouri) at 1:200, goat anti-TEX14 at 1:300, rabbit anti-MKLP1 at 1:500, rabbit anti-MgcRacGAP at 1:300, rabbit anti-anillin at 1:200, rabbit anti-SEPT2 1:500, rabbit anti-SEPT7 at 1:500, rabbit anti-SEPT9 at 1:500. Alexa 488, 555, and 694 secondary antibodies were purchased from Molecular Probes, Eugene, OR. Samples were mounted with Prolong Gold mounting media with DAPI (Invitrogen) and examined on a Zeiss (Carl Zeiss MicroImaging, Thornwood, NY) Axiovert s100 2TV. When required, deconvolution was performed with softWoRx v3.3.6 (Applied Precision, Issaquah, WA).

Proteomic Analysis

Eighty micrograms of the P3 fraction was run in one lane of a 1mm X 10 lane NuPAGE 4–12% Bis-Tris Gel (Invitrogen, Carlsbad, California) and stained with Brilliant Blue R (Sigma). The lane was cut using sterile technique into 10 approximately equally stained pieces, and the pieces were place in 1.5ml microcentrifuge tubes (Eppendorf). Gel slices were washed in the tube 3 times with 50% acetonitrile in HPLC grade water and sent on dry ice to the Beth Israel Deaconess Medical Center Mass Spectrometry Core Facility, Boston, MA, care of Dr. J. Asara, for protein extraction and LC/MS/MS analysis.

Results and Discussion

Enrichment of Mammalian Germ Cell Intercellular Bridges

To identify new mammalian intercellular bridge components and how germ cell bridges form, we needed to obtain an enriched fraction of intercellular bridges from mammalian germ cells. Structurally, the intercellular bridge is composed predominantly of an actin-containing (Russell et al., 1987), electron dense “bridge density” that lines the inner walls of the channel (Burgos and Fawcett, 1955). The appearance of this structure is very similar to the actin rich, neuronal postsynaptic densities which line the dendritic side of the synaptic cleft (Cotman and Taylor, 1972). The physical dimensions of newly formed germ cell intercellular bridges are similar to the cleavage furrows and midbodies enriched by the protocol of Mullins and McIntosh (Mullins and McIntosh, 1982). Proteomic analysis of midbodies enriched by this protocol identified several new midbody components (Skop et al., 2004). Likewise, enrichment protocols have been developed (Cotman and Taylor, 1972) which led to the proteomic identification of many postsynaptic density components (Walikonis et al., 2000). Structural similarities between the intercellular bridge, the midbody, and the neuronal postsynaptic density, suggested that an enrichment protocol for intercellular bridges could be developed based on these other studies. Unlike the midbody protocol (Mullins and McIntosh, 1982; Skop et al., 2004), which utilizes cultured cells, the postsynaptic density protocol uses animal tissue as the starting material (Cotman and Taylor, 1972; Walikonis et al., 2000).

Since *in vitro* culturing conditions for differentiated germ cells are still being developed, post-natal day 16 mouse testes were selected as the starting material. A higher proportion of germ cells are dividing in young mice resulting in large numbers of newly formed intercellular bridges. Since no new intercellular bridges are formed after meiosis, a higher density of intercellular bridges was postulated to be present in 16-day-old testes (Bellve et al., 1977). Higher rates of cell division should also result in more of bridges in the early stages of formation compared to adult mice. Furthermore, mature germs cells contain many contaminating cytoskeletal structures (e.g., the manchette and sperm tail) which are absent at 16 days. The simple, rapid enrichment procedure is outlined in Figure 1A and described in detail in the Materials and Methods. Briefly, seminiferous tubules are removed from the testis and disrupted with a glass-Teflon homogenizer in isotonic sucrose buffer. Large debris and most nuclei are removed in an initial slow speed spin (720g). A higher force spin (3,500g) collects the remaining intercellular bridges. This second pellet after washing (P2), is resuspended in a hypotonic, 0.5% Triton X-100 solution and incubated at 4°C. The heavy Triton X-100 insoluble fraction is collected at 3,500g. This final fraction, after a gentle wash, is referred to as P3. In three independent experiments, a starting mass of 27.1±6.3g yielded 1.65±0.67g of P2 and 0.134±0.095g of P3. TEX14 was enriched 2.3±0.2 fold in P2 and 29.1±1.95 fold in P3 over initial total levels by quantitative western analysis (Figure 1B, TEX14). Immunofluorescence of the P3 pellet using an anti-TEX14 antibody shows large numbers of intercellular bridges, many in the shape of rings (Fig. 1D)

Centralspindlin is a Component of the Mammalian Intercellular Bridge

Proteins from the P3 fraction were identified by 1D-PAGE/LC/MS/MS analysis. A total of 586 groups were identified in the P3 fraction. As in previous work (Skop et al., 2004), the number of peptides in a group was used to narrow the results. One hundred twenty seven proteins with at least 5 unique peptides were identified and categorized (see supplementary information, Table). Since the enriched intercellular bridges were likely in various stages of development, some components may have been underrepresented and, therefore, inappropriately excluded from this group if they are transient in the developing intercellular bridge. For this reason, proteins with a known role in cytokinesis were given special consideration (see supplementary information, Table). TEX14 was identified by a group of 30 peptides covering 29.0% of the total sequence (Supplementary Table and Supplementary Figure 1). Since we hypothesized that some components involved in mammalian intercellular bridge formation are cytokinesis components which remain physically associated with the intercellular bridge, we were particular interested in any midbody components identified (see supplementary information, Table, bold text).

Midbody components MKLP1 (Kuriyama et al., 2002; Matuliene and Kuriyama, 2004) and MgcRacGAP (Arar et al., 1999), which form the centralspindlin complex (Mishima et al., 2002), were identified in the proteomic analysis. A group of 23 peptides covered 30.0% of MKLP1 (see supplementary information, Table and Figure S1), and a group of 9 peptides covered 28.4% of MgcRacGAP (see supplementary information, Table and Figure 1). Western blot analyses showed bands for MKLP1 at around 100kD and MgcRacGAP at 70kD which co-enrich similarly to TEX14 in the P2 and P3 fractions (Fig. 1B) In contrast the cis-Golgi matix protein GM130, a Golgi protein not found in the intercellular bridge, is removed during the enrichment process (Fig. 1B). To confirm that TEX14 was required for enrichment of MKLP1 and MgcRacGAP, we performed an identical intercellular bridge prep on *Tex14* knockout testes which lack intercellular bridges (Greenbaum et al., 2006). In contrast to control testes, MKLP1 and MgcRacGAP are absent from the P3 fraction of *Tex14* knockout testes (Fig. 1C). Co-enrichment with TEX14, dependent on the presence of TEX14, suggested that MKLP1 and MgcRacGAP are components of the intercellular bridge. The nuclear protein synaptonemal complex central element protein 1 (SYCE1), a contaminant not present in the intercellular bridge, is used as a loading control.

Since TEX14, MKLP1, and MgcRacGAP co-enriched in the intercellular bridge preparation, we used immunofluorescence to determine if they co-localize in the testis. Immunofluorescence of 14 day-old control testis shows that both MKLP1 (Fig. 2A, top row) and MgcRacGAP (Fig. 2A, bottom row) co-localize with TEX14 in the intercellular bridge. Intercellular bridges were not found by MKLP1 immunofluorescence of 14 day-old *Tex14* knockout testis (Fig. 2B, left panel); however, midbodies are able to form in the absence of TEX14, and MKLP1 correctly localizes to the midbody matrix, identified as the midzone of the midbody (Fig. 2B, green) which excludes tubulin immunofluorescence (Fig. 2B, red) (Mullins and McIntosh, 1982). Since loss of TEX14 does not result in multinucleated germ cells (Greenbaum et al., 2006), the midbody is somehow resolved in differentiating spermatogonia or spermatocytes, either through normal abscission or an alternative process, allowing for somatic cell-like cytokinesis to occur. The co-localization of MKLP1 (Fig. 2A and 2C, top row) and MgcRacGAP (Fig. 2A and 2C, bottom row) with TEX14 in the intercellular bridge is conserved from mice to man, suggesting an evolutionarily conserved mechanism of intercellular bridge formation. This mechanism likely involves the direct interaction of TEX14 with the MKLP1 in the intercellular bridge, since TEX14 was found to interact with MKLP1 in a targeted yeast-two-hybrid assay (see Supplementary Figure 2).

TEX14 is a Germ Cell Cytokinesis Protein Localized by Somatic Cell Factors

While TEX14 is not required for formation of germ cell midbodies (Fig. 2B), it is incorporated into the contractile ring by telophase (Fig. 3A). In anaphase, MKLP1 localizes to the midzone of the mitotic spindle (Fig. 3A, left column), while TEX14 remains diffuse in the cytoplasm. Both MKLP1 and TEX14 localize to the contractile ring in early telophase (Fig. 3A, middle column) and the midzone of the midbody in late telophase (Fig. 3A, right column). Lateral and angled views of the midbody demonstrate that TEX14 and MKLP1 do not co-localize in the midbody matrix. Instead, TEX14 joins the midbody matrix structure by forming an inner ring which does not contain MKLP1. A targeted yeast-two-hybrid experiment demonstrates that TEX14 is capable of self-interaction (see Supplementary Figure 2), which may be important for formation the inner ring.

To determine if other germ cell specific factors are required for TEX14 localization and intercellular bridge formation, we expressed TEX14 in two somatic cell lines. TEX14 localized to the midbody matrix in dividing CHO and HeLa cells (Fig. 3B and C). This localization is identical to the germ cell localization of TEX14 *in vivo* (Fig. 2 and 3A), demonstrating that no germ cell-specific factors are required for TEX14 localization. Thus, TEX14 directly interacts with somatic cell cytokinesis components. Despite correct localization, TEX14 is not sufficient to form stable intercellular bridges in somatic cells. TEX14 is occasionally seen in residual bodies (Fig. 3D) suggesting that other testis-specific components are required to prevent abscission.

Septins and Centralspindlin Form an Outer Ring in Early Intercellular Bridges

Previous work has demonstrated that mature intercellular bridges grow in diameter as germ cells develop. For example, electron microscopy has shown that type A spermatogonial bridges have a diameter of 1um. The bridges expand to 1.5um in spermatocytes and 2–3um in spermatids (Weber and Russell, 1987). We found that ring growth is also a characteristic of the transition from midbody to mature intercellular bridge. Midbodies joining spermatogonia or spermatocytes initially contain an inner TEX14 ring with an outer centralspindlin ring (Fig. 3A). After the tubulin rich central spindle between these cells is disassembled, TEX14 continues to maintain a ring within the outer centralspindlin ring in the early bridge (Fig. 4A). As the bridge matures, the TEX14 inner ring grows in diameter and begins to “invade” the outer centralspindlin ring, eventually merging with it (Fig. 4A). Thus, during early bridge formation, there exists an inner TEX14 rim and an outer centralspindlin rim. The TEX14 ring completes its merger with the centralspindlin ring in mature bridges (Fig. 2A and Fig. 4A), and the mature bridges expand as previously describe, reaching up to 3um in spermatids (Weber and Russell, 1987).

Female *Drosophila* intercellular bridges also expand during development and, like mammalian bridges, are actin rich (Robinson and Cooley, 1996). These observations suggest that male intercellular bridge formation in mammals may actually be more analogous to the process in *Drosophila* females than the process in males, where bridge formation is largely septin-based (Hime et al., 1996). To see if there was any molecular similarity to male *Drosophila* intercellular bridge formation, we examined the septins. Three of the 12 possible mammalian septins (Kinoshita, 2003) were identified in the enriched bridge fraction: SEP2, SEP7 and SEP9. Anillin, which is also in male *Drosophila* bridges, was not identified in the enriched fraction.

Septins are required for somatic cell cytokinesis in some cell types (Glotzer, 2005) and are capable of self assembly into rings (Kinoshita et al., 2002). They also interact with anillin (Field and Alberts, 1995; Kinoshita et al., 2002), a protein that localizes early to the cleavage furrow (Field and Alberts, 1995), but is not essential until late events in cytokinesis (Somma

et al., 2002; Straight et al., 2005). In germ cell cytokinesis, male *Drosophila* bridges contain three septins (Peanut, SEP1, and SEP2) and anillin (Hime et al., 1996). In female *Drosophila*, a fraction of the bridges contain Peanut (Adam et al., 2000; Djagaeva et al., 2005), although Peanut is not required for cytokinesis (Adam et al., 2000). SEP1 and SEP2 have not been identified as components of the female *Drosophila* intercellular bridge (Djagaeva et al., 2005). Anillin localizes to the female intercellular bridge only during early bridge formation (Field and Alberts, 1995).

As mentioned, three septins, SEPT2, SEPT7, and SEPT9, but not anillin, were identified in the proteomics screen (see supplementary information, Table, and Figure 1). By BLAST alignment, SEPT2 and SEPT7 are most similar to *Drosophila* SEP1 and Peanut, respectively, while SEPT9 aligns almost equally well to both SEP1 and Peanut. All three septins identified in the proteomics were found to enrich with intercellular bridges by western blot analysis (Fig. 4C). Additionally, all three septins were found to localize to the outer ring of early developing intercellular bridges in mouse testis (Fig. 4B). Septins were not seen in the midbody matrix prior to disassembly of the central spindle, nor were they found in mature intercellular bridges. SEPT7 and anillin were also found to localize to the cleavage furrow and midbody (Field and Alberts, 1995). SEPT7 and anillin localize to cables parallel to the spindle axis early in cytokinesis (data not shown), and in telophase they localize to cables perpendicular to the cleavage axis in a “ring” (Fig. 4B). In contrast to male and female *Drosophila*, anillin is not in the intercellular bridge in mammals.

To further examine the stage of septin involvement in the developing intercellular bridge, the diameter of the TEX14 inner ring in SEPT9 containing bridges was measured in spermatogonia. The diameter of the inner ring in these bridges was 0.68 um ± 0.05 (n=10). This was compared to the diameter of TEX14 in bridges where TEX14 had joined the outer MKLP1 ring, 1.24 um ± 0.06 (n=10). These represent two different populations of intercellular bridges ($p=1.2\times10^{-6}$; T-Test). TEX14 and MKLP1 also co-localize in all spermatid bridges, further supporting that co-localization and a TEX14 diameter >1um defines a mature intercellular bridge. Conversely, a smaller TEX14 diameter and the presence of septins suggest an early stage of bridge formation. Septins were not observed in bridges >1um. In the developing spermatogonial bridges containing SEPT9, the TEX14 ring diameter was found to range from 0.49 um to 0.87 um. The length of time it takes for the TEX14 ring to expand, and how long septins remain in the early bridge remains unknown and may vary between bridges and cell type.

Together, the proteins identified in this study describe several distinct molecular stages in mammalian germ cell intercellular bridge development during spermatogenesis (Figure 5). Initially in anaphase, TEX14 is distributed diffusely in the cytoplasm, and germ cell cytokinesis seems identical to somatic cells. By early telophase, however, TEX14 has begun to localize to the inner surface of the contractile ring, just inside centralspindlin, SEPT7 and Anillin (Fig. 5, Early Telophase). In late telophase, TEX14 forms an inner ring in the midbody matrix, completely inside the outer ring containing centralspindlin. Meanwhile, anillin and SEPT7 have moved to the flanks of the midbody, lateral to the matrix (Fig. 5, Midbody). Transitioning from the midbody to an early intercellular bridge requires TEX14. After the central spindle disassembles, anillin is no longer present in the developing intercellular bridge. SEPT7, in contrast, returns to the outer ring of the early intercellular bridge and is joined by SEPT2 and SEPT9 (Fig. 5, Early ICB). Centralspindlin remains in the outer ring, completely separate from the inner TEX14 ring. As the early intercellular bridge matures, the septins are removed, and the inner TEX14 ring expands outward to a diameter of at least 1um and integrates into the outer centralspindlin ring until the two rings completely merge (Fig. 5, Mature ICB). A targeted yeast-two-hybrid assay shows that TEX14 interacts strongly with MKLP1, but very weakly with MgcRacGAP (Supplementary Figure 2). This interaction could be important as the inner

TEX14 ring joins the outer centralspindlin ring. The mature bridge greatly increases in diameter as the cells differentiate into spermatids (Fig. 5, Spermatid ICB). This is accompanied by the removal of Keratin 5, a previously identified spermatocyte bridge marker (Tres et al., 1996), and the addition of Protocadherin Alpha3 (Johnson et al., 2004) to spermatid bridges. Additionally, MgcRacGAP is no longer seen in the bridges of spermatids (data not shown). It is possible that MKLP1 is the only essential component of the centralspindlin complex in the spermatid intercellular bridge. MKLP1 organizes the cytoskeleton in the neuronal dendrites (Ferhat et al., 1998), while no similar role has been described for MgcRacGAP. Additionally, MKLP1, but not the MgcRacGAP homologue, has been identified as a component of *Drosophila* intercellular bridges (Carmena et al., 1998;Minestrini et al., 2002). Thus, compared to MgcRacGAP, MKLP1 may have a unique structural function after initial formation of the intercellular bridge.

In conclusion, this work shows that TEX14 is essential for the conversion of the midbody into a germ cell intercellular bridge. Without TEX14, the intercellular bridge cannot incorporate septins, and likely other proteins, after the central spindle breaks down and the daughter cells separate. Although TEX14 localizes correctly to the midbody of somatic cells, it is not sufficient to create a stable intercellular bridge. TEX14-containing intercellular bridges lacking central spindles are never observed in somatic cells. Other germ cell specific factors, either recruited by TEX14 or localizing independently, are likely required to prevent abscission and allow a stable intercellular bridge to be maintained after loss of the central spindle. While some of these factors may be identified here, others may not have been enriched, since some known bridge proteins were not identified. Interactions that cannot withstand hypotonic conditions or Triton X-100 may have resulted in the loss of some bridge proteins. Complementary biochemical approaches could prove helpful. Further work to identify novel spermatid bridge components is also important given the proposed roles of intercellular bridges in haploid cells (Braun et al., 1989). As mentioned previously, the abundance of cytoskeletal structures in mature germ cells complicates the approach presented here. Finally, since the conclusion to germ cell cytokinesis is mechanistically distinct from somatic cell cytokinesis, and intercellular bridges are essential for male fertility (Greenbaum et al., 2006) and conserved in humans, TEX14 and other unique components of the germ cell intercellular bridge may provide safe and effective contraceptive targets for men.

Supplementary Material

Refer to Web version on PubMed Central for supplementary material.

Acknowledgments

We thank Ms. S. Baker for her expert assistance in manuscript formatting, Drs. L. YuLee and Y. Kurasawa for critical reading of the manuscript, and Drs. M. Kinoshita (Kyoto University Graduate School of Medicine, Kyoto, Japan) for anti-SEPT7 and anti-SEPT9, K. Nagata (Aichi Human Service Center, Kamiyacho, Japan) for anti-SEPT9, T. Kitamura (University of Tokyo, Tokyo, Japan) for anti-MgcRacGAP antibodies, G. Fang (Stanford, Stanford, CA) for anti-MgcRacGAP antibodies and anti-anillin antibodies, G. Warren (Yale, Newhaven, CT) for the anti-GM130 and R. Kuriyama (University of Minnesota, Minneapolis, MN) for the anti-MKLP1 antibodies. These studies were supported in part by the National Institutes of Health Cooperative Centers Program in Reproduction Research (HD07495 to M.M.M). M.P.G. is a student in the Medical Scientist Training Program (T32GM07330) and has been supported by NIMH NRSA grant F30MH066542, a Hudson Scholarship, and the BRASS Foundation.

References

Adam JC, Pringle JR, Peifer M. Evidence for functional differentiation among Drosophila septins in cytokinesis and cellularization. Mol Biol Cell 2000;11:3123–35. [PubMed: 10982405]

Arar C, Ott MO, Toure A, Gacon G. Structure and expression of murine mgcRacGAP: its developmental regulation suggests a role for the Rac/MgcRacGAP signalling pathway in neurogenesis. Biochem J 1999;343(Pt 1):225–30. [PubMed: 10493933]

Bellve AR, Cavicchia JC, Millette CF, O'Brien DA, Bhatnagar YM, Dym M. Spermatogenic cells of the prepuberal mouse. Isolation and morphological characterization. J Cell Biol 1977;74:68–85. [PubMed: 874003]

Braun RE, Behringer RR, Peschon JJ, Brinster RL, Palmiter RD. Genetically haploid spermatids are phenotypically diploid. Nature 1989;337:373–6. [PubMed: 2911388]

Brill JA, Hime GR, Scharer-Schuksz M, Fuller MT. A phospholipid kinase regulates actin organization and intercellular bridge formation during germline cytokinesis. Development 2000;127:3855–64. [PubMed: 10934029]

Burgos MH, Fawcett DW. Studies on the fine structure of the mammalian testis. I. Differentiation of the spermatids in the cat (Felis domestica). J Biophys Biochem Cytol 1955;1:287–300. [PubMed: 13242594]

Carmena M, Riparbelli MG, Minestrini G, Tavares AM, Adams R, Callaini G, Glover DM. Drosophila polo kinase is required for cytokinesis. J Cell Biol 1998;143:659–71. [PubMed: 9813088]

Cotman CW, Taylor D. Isolation and structural studies on synaptic complexes from rat brain. J Cell Biol 1972;55:696–711. [PubMed: 4656707]

Djagaeva I, Doronkin S, Beckendorf SK. Src64 is involved in fusome development and karyosome formation during Drosophila oogenesis. Dev Biol 2005;284:143–56. [PubMed: 15979065]

Dodson GS, Guarnieri DJ, Simon MA. Src64 is required for ovarian ring canal morphogenesis during Drosophila oogenesis. Development 1998;125:2883–92. [PubMed: 9655810]

Dym M, Fawcett DW. Further observations on the numbers of spermatogonia, spermatocytes, and spermatids connected by intercellular bridges in the mammalian testis. Biol Reprod 1971;4:195–215. [PubMed: 4107186]

Fabbro M, Zhou BB, Takahashi M, Sarcevic B, Lal P, Graham ME, Gabrielli BG, Robinson PJ, Nigg EA, Ono Y, Khanna KK. Cdk1/Erk2- and Plk1-dependent phosphorylation of a centrosome protein, Cep55, is required for its recruitment to midbody and cytokinesis. Dev Cell 2005;9:477–88. [PubMed: 16198290]

Fawcett DW, Ito S, Slautterback D. The occurrence of intercellular bridges in groups of cells exhibiting synchronous differentiation. J Biophys Biochem Cytol 1959;5:453–60. [PubMed: 13664686]

Ferhat L, Kuriyama R, Lyons GE, Micales B, Baas PW. Expression of the mitotic motor protein CHO1/MKLP1 in postmitotic neurons. Eur J Neurosci 1998;10:1383–93. [PubMed: 9749792]

Field CM, Alberts BM. Anillin, a contractile ring protein that cycles from the nucleus to the cell cortex. J Cell Biol 1995;131:165–78. [PubMed: 7559773]

Fielding AB, Schonteich E, Matheson J, Wilson G, Yu X, Hickson GR, Srivastava S, Baldwin SA, Prekeris R, Gould GW. Rab11-FIP3 and FIP4 interact with Arf6 and the exocyst to control membrane traffic in cytokinesis. Embo J 2005;24:3389–99. [PubMed: 16148947]

Glotzer M. The molecular requirements for cytokinesis. Science 2005;307:1735–9. [PubMed: 15774750]

Greenbaum MP, Yan W, Wu MH, Lin YN, Agno JE, Sharma M, Braun RE, Rajkovic A, Matzuk MM. TEX14 is essential for intercellular bridges and fertility in male mice. Proc Natl Acad Sci U S A 2006;103:4982–7. [PubMed: 16549803]

Gromley A, Yeaman C, Rosa J, Redick S, Chen CT, Mirabelle S, Guha M, Sillibourne J, Doxsey SJ. Centriolin anchoring of exocyst and SNARE complexes at the midbody is required for secretory-vesicle-mediated abscission. Cell 2005;123:75–87. [PubMed: 16213214]

Hedges SB. The origin and evolution of model organisms. Nat Rev Genet 2002;3:838–49. [PubMed: 12415314]

Hime GR, Brill JA, Fuller MT. Assembly of ring canals in the male germ line from structural components of the contractile ring. J Cell Sci 1996;109 (Pt 12):2779–88. [PubMed: 9013326]

Huckins C. The spermatogonial stem cell population in adult rats. I. Their morphology, proliferation and maturation. Anat Rec 1971;169:533–57. [PubMed: 5550532]

Huckins C, Oakberg EF. Morphological and quantitative analysis of spermatogonia in mouse testes using whole mounted seminiferous tubules, I. The normal testes. Anat Rec 1978;192:519–28. [PubMed: 736272]

Johnson KJ, Zecevic A, Kwon EJ. Protocadherin alpha3 acts at sites distinct from classic cadherins in rat testis and sperm. Biol Reprod 2004;70:303–12. [PubMed: 14522826]

Kinoshita M. The septins. Genome Biol 2003;4:236. [PubMed: 14611653]

Kinoshita M, Field CM, Coughlin ML, Straight AF, Mitchison TJ. Self- and actin-templated assembly of Mammalian septins. Dev Cell 2002;3:791–802. [PubMed: 12479805]

Kuriyama R, Gustus C, Terada Y, Uetake Y, Matuliene J. CHO1, a mammalian kinesin-like protein, interacts with F-actin and is involved in the terminal phase of cytokinesis. J Cell Biol 2002;156:783–90. [PubMed: 11877456]

Low SH, Li X, Miura M, Kudo N, Quinones B, Weimbs T. Syntaxin 2 and endobrevin are required for the terminal step of cytokinesis in mammalian cells. Dev Cell 2003;4:753–9. [PubMed: 12737809]

Matuliene J, Kuriyama R. Role of the midbody matrix in cytokinesis: RNAi and genetic rescue analysis of the mammalian motor protein CHO1. Mol Biol Cell 2004;15:3083–94. [PubMed: 15075367]

Minestrini G, Mathe E, Glover DM. Domains of the Pavarotti kinesin-like protein that direct its subcellular distribution: effects of mislocalisation on the tubulin and actin cytoskeleton during Drosophila oogenesis. J Cell Sci 2002;115:725–36. [PubMed: 11865028]

Mishima M, Kaitna S, Glotzer M. Central spindle assembly and cytokinesis require a kinesin-like protein/RhoGAP complex with microtubule bundling activity. Dev Cell 2002;2:41–54. [PubMed: 11782313]

Moens PB, Hugenholtz AD. The arrangement of germ cells in the rat seminiferous tubule: an electron-microscope study. J Cell Sci 1975;19:487–507. [PubMed: 1206045]

Mullins JM, McIntosh JR. Isolation and initial characterization of the mammalian midbody. J Cell Biol 1982;94:654–61. [PubMed: 7130277]

Ren HP, Russell LD. Clonal development of interconnected germ cells in the rat and its relationship to the segmental and subsegmental organization of spermatogenesis. Am J Anat 1991;192:121–8. [PubMed: 1759679]

Robinson DN, Cant K, Cooley L. Morphogenesis of Drosophila ovarian ring canals. Development 1994;120:2015–25. [PubMed: 7925006]

Robinson DN, Cooley L. Stable intercellular bridges in development: the cytoskeleton lining the tunnel. Trends Cell Biol 1996;6:474–9. [PubMed: 15157506]

Russell LD, Vogl AW, Weber JE. Actin localization in male germ cell intercellular bridges in the rat and ground squirrel and disruption of bridges by cytochalasin D. Am J Anat 1987;180:25–40. [PubMed: 3310595]

Skop AR, Liu H, Yates J 3rd, Meyer BJ, Heald R. Dissection of the mammalian midbody proteome reveals conserved cytokinesis mechanisms. Science 2004;305:61–6. [PubMed: 15166316]

Somma MP, Fasulo B, Cenci G, Cundari E, Gatti M. Molecular dissection of cytokinesis by RNA interference in Drosophila cultured cells. Mol Biol Cell 2002;13:2448–60. [PubMed: 12134082]

Straight AF, Field CM, Mitchison TJ. Anillin binds nonmuscle myosin II and regulates the contractile ring. Mol Biol Cell 2005;16:193–201. [PubMed: 15496454]

Tres LL, Rivkin E, Kierszenbaum AL. Sak 57, an intermediate filament keratin present in intercellular bridges of rat primary spermatocytes. Mol Reprod Dev 1996;45:93–105. [PubMed: 8873075]

Ventela S, Toppari J, Parvinen M. Intercellular organelle traffic through cytoplasmic bridges in early spermatids of the rat: mechanisms of haploid gene product sharing. Mol Biol Cell 2003;14:2768–80. [PubMed: 12857863]

Walikonis RS, Jensen ON, Mann M, Provance DW Jr, Mercer JA, Kennedy MB. Identification of proteins in the postsynaptic density fraction by mass spectrometry. J Neurosci 2000;20:4069–80. [PubMed: 10818142]

Weber JE, Russell LD. A study of intercellular bridges during spermatogenesis in the rat. Am J Anat 1987;180:1–24. [PubMed: 3661461]

Yates JR 3rd, Gilchrist A, Howell KE, Bergeron JJ. Proteomics of organelles and large cellular structures. Nat Rev Mol Cell Biol 2005;6:702–14. [PubMed: 16231421]

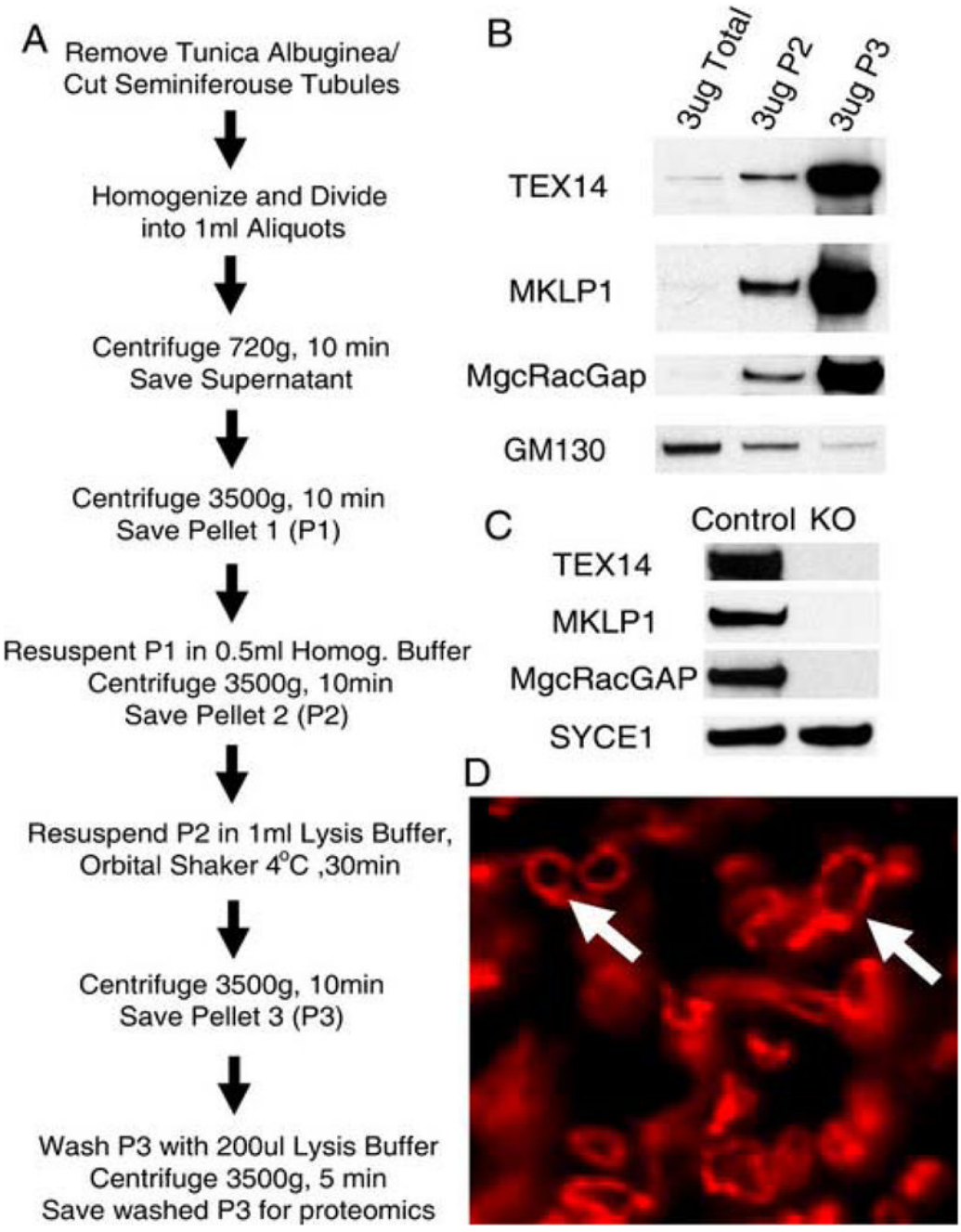

Fig. 1. Enrichment of mammalian intercellular bridges

(A) Following homogenization, a series of centrifugation steps and a Triton X-100 treatment were used to enrich the germ cell intercellular bridge. (B) Components of the centralspindlin complex co-enrich with TEX14 and intercellular bridges. (C) Enrichment of centralspindlin occurs in control testes, but not in the testes of *Tex14* knockout (KO) mice. (D) Intercellular bridges, often retaining their 'ring' shape (arrows), contain TEX14 (red) and are abundant in the final pellet, P3.

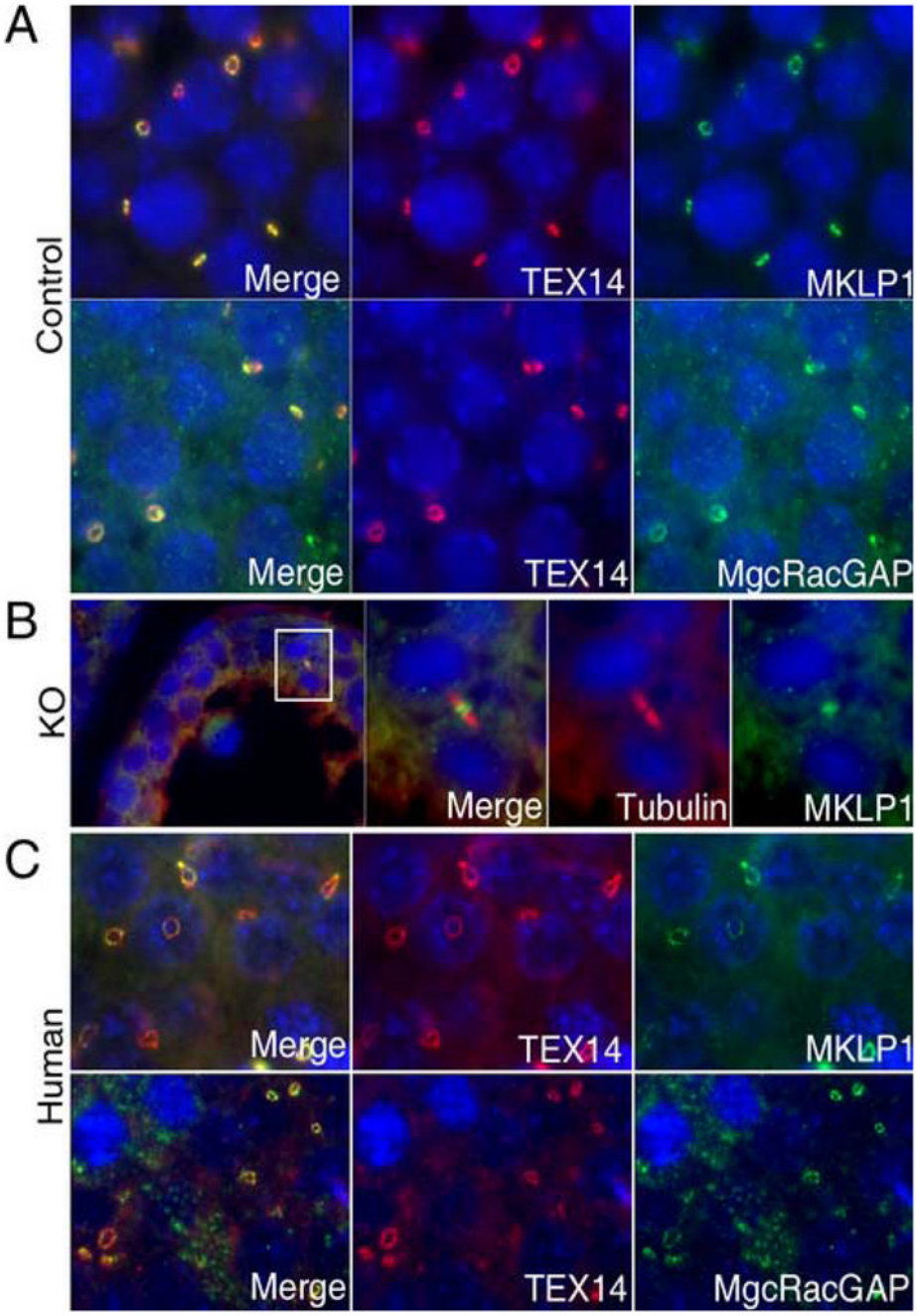

Fig. 2. Intercellular bridge localization of MKLP1 and MgcRacGAP in control mouse and human testis, but not *Tex14* knockout 14 day-old testis

(A) MKLP1 and MgcRacGAP (green) co-localize with TEX14 (red) in the intercellular bridges of a control testis, but not a *Tex14* KO testis (B, left panel). (B) Tubulin (red) and MKLP1 (green) demonstrate that midbodies form during late telophase between dividing germ cells in *Tex14* KO testis. (C) MKLP1 and MgcRacGAP (green) also co-localize with TEX14 (red) in a normal human testis.

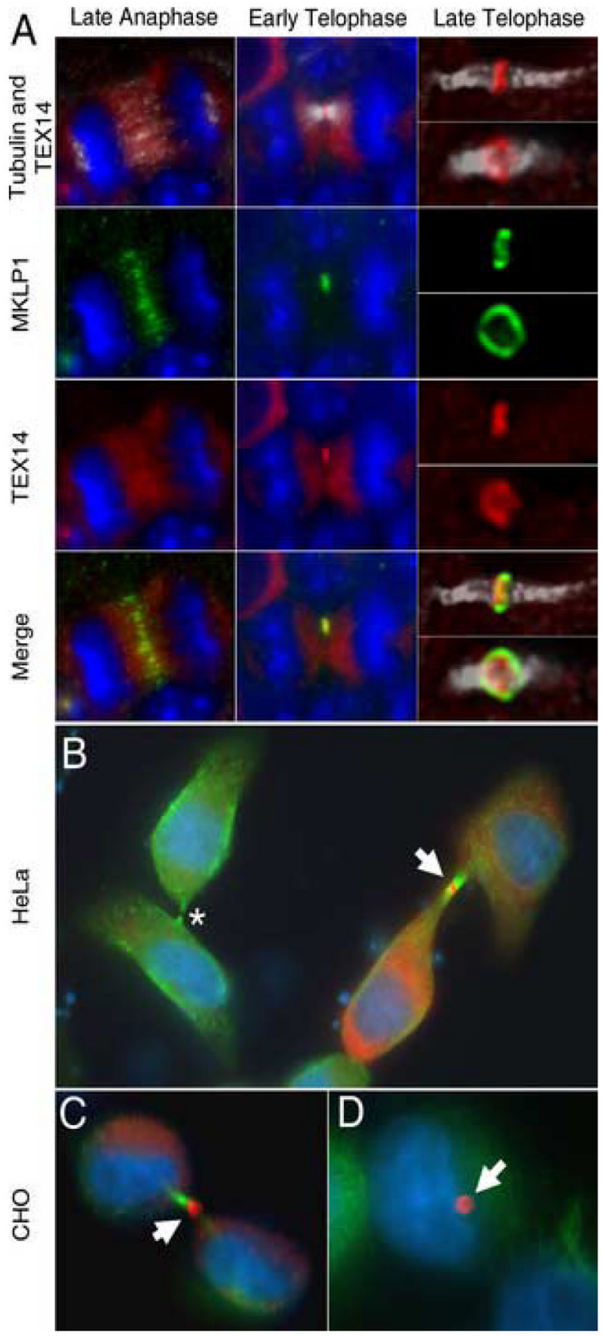

Fig. 3. TEX14 and MKLP1 localization during cytokinesis

(A) Tubulin (white) identifies the mitotic spindles of dividing germ cells in an 8-day-old testis. The spindle and nuclear structure (DAPI, blue) identify the stage of cytokinesis as late anaphase (left column), early telophase (middle column), and late telophase (right column). TEX14 (red) has cytoplasmic localization until early telophase when it begins to localize to the spindle midzone. TEX14 forms an “inner ring” inside the centralspindlin ring, shown here with two views of midbodies from different angles during late telophase. TEX14 (red) also localizes to the midbody of HeLa (B, arrow) and CHO (C) cells when ectopically expressed by transfection (Tubulin, green; DAPI, blue). No midbody staining is observed in untransfected cells (B,

asterisk). (D) CHO cell showing residual bodies containing TEX14 (red) are occasionally observed.

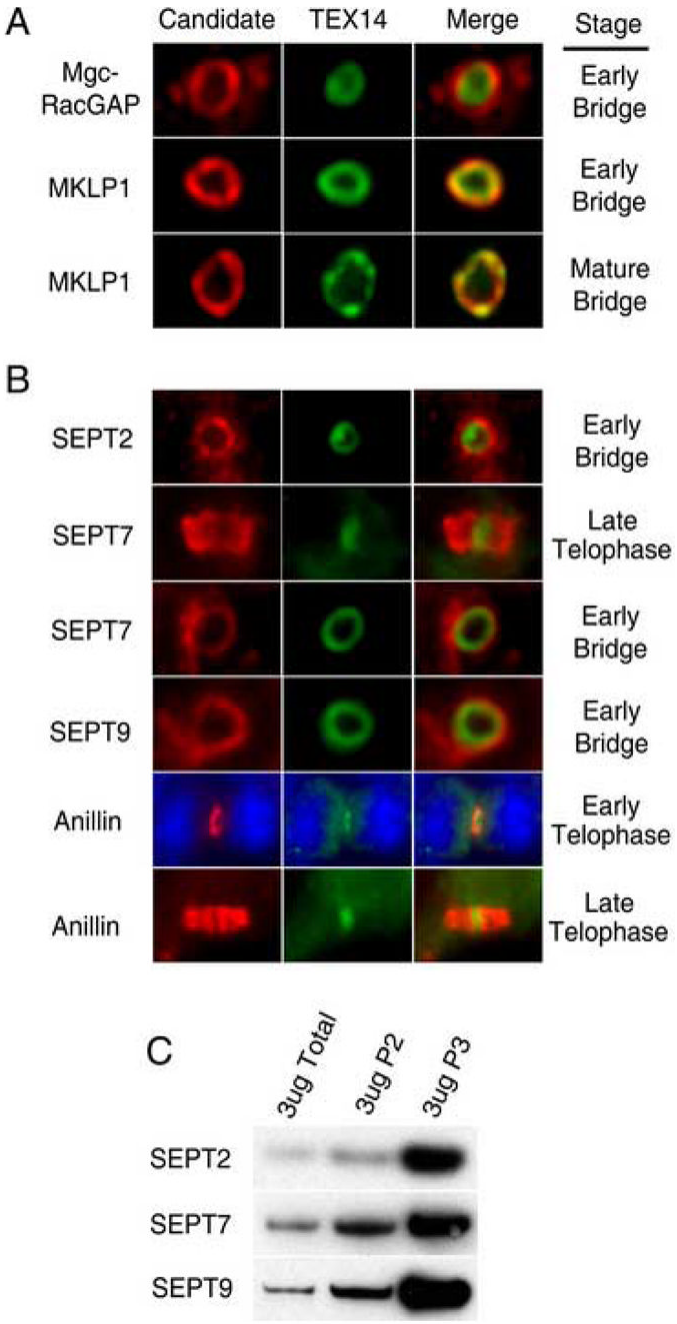

Fig. 4. Localization of novel intercellular bridge candidates during intercellular bridge development in germ cells

(A) MgcRacGAP and MKLP1 (red) in the outer ring surround the inner TEX14 ring in early intercellular bridges. As the intercellular bridge matures, TEX14 incorporates into the outer ring. In mature bridges there is only one ring containing centralspindlin (MKLP1, red) and TEX14 (green), but no septins. (B) All three septins (red) form an outer ring around a TEX14 (green) containing inner ring during the early development of intercellular bridges. Anillin (red) and SEPT7 are present at cytokinesis, but only SEPT7 enters the intercellular bridge. (C) SEPT2, SEPT7, and SEPT9 enrich similarly to TEX14 in P2 and P3 when intercellular bridges are enriched.

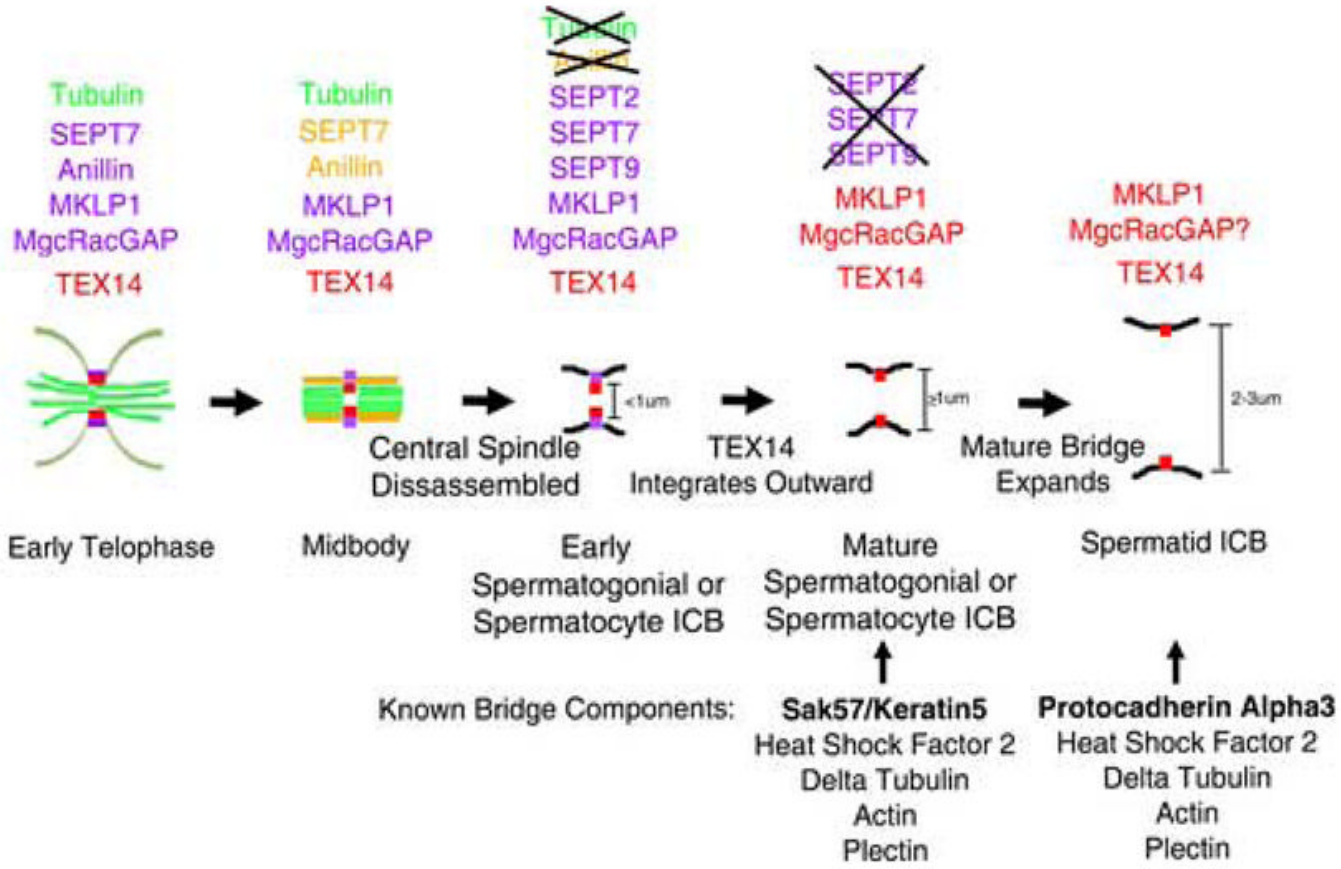

Fig. 5. Molecular model for mammalian germ cell intercellular bridge development

See text for details. In early telophase, TEX14 begins to localize to the cleavage furrow inside the SEPT7, anillin, and centralspindlin ring. At late telophase, TEX14 forms an inner ring inside the midbody matrix, while centralspindlin is excluded and localizes to the outer midbody matrix ring. SEPT7 and anillin are not present in the midbody matrix but localize to the lateral parts of the midbody with the tubulin spindle. Maintenance of the intercellular bridge, while the central spindle disassembles, is dependant on TEX14. After the central spindle is gone the bridge goes through a transitional state. In the early bridges of spermatogonia and spermatocytes, TEX 14 is maintained in the inner ring, while SEPT2, SEPT7, and SEPT9 are added to the outer ring with centralspindlin. As the ring matures, TEX14 incorporates into the outer ring, eventually co-localizing with centralspindlin. The diameter of the TEX14 ring in early bridges, prior to co-localization, is less than 1um. The septins leave the outer ring as the intercellular bridge matures and are not present in mature spermatogonial and spermatocyte bridges, which are 1um or greater in diameter. The diameter of the intercellular bridge dramatically increases in spermatids to 2–3um. Some previously described molecular components of the intercellular bridge change at this point (Keratin5 and Protocadherin Alpha3), while others are apparently maintained (Heat Shock Factor 2, Delta Tubulin, and Actin). TEX14 and MKLP1 are maintained in all intercellular bridges including spermatids. MgcRacGAP is not visible in spermatid bridges but may be obscured by relatively high background levels. (ICB; Intercellular Bridge)